Vector Field Tomography by Electron Holography

Ruriko Tsuneta[1], Masaki Ikeda[1], Shiano Ono[1], Miyuki Yamane[1], Akira Sugawara[1], Ken Harada[1] and Masanari Koguchi[1]

[1]Central Research Laboratory, Hitachi Ltd., Hatoyama, Saitama 350-0395, JAPAN

Electron tomography has rapidly developed in the last decade with the progress of modern computationally controlled electron microscopy and the development of algorithms for the Radon transformation and image processing with interpolation [1]. On the other hand, electron holography has been one of the standard techniques for observing phase maps of electron waves since the commercialization of the field emission electron gun. The technological combination of tomography and holography has also led to elucidation of the distributions of the mean inner potential of materials [2]. In the case of the magnetic field, the component B_y parallel to the rotation axis (see Fig. 1) can be calculated from the phase shift $\Delta\phi_y$ by using the conventional tomography algorithm [3], but the other two components (B_x, B_z) perpendicular to the rotation-axis cannot be calculated, because the two components are mixed together with a rotation angle θ. In the case of a magnetic field in free space, however, the phase shift $\Delta\phi_\theta$ projected to the optical axis is described simply [4] as Eq. 2, for which B_x and B_z can be separated.

$$\Delta\phi_y \propto \int_{-\infty}^{+\infty} B_y \, dl \tag{1}$$

$$\Delta\phi_\theta \propto \int_{-\infty}^{+\infty} (B_x \cos\theta + B_z \sin\theta) \, dl \tag{2}$$

Figure 1 shows a schematic diagram of the tomography/holography experiment. A thin magnetic pillar made of C/CoFeB/SiO2 was prepared with a focused ion beam machine (see Fig. 2(a)) and mounted on the 360° rotation axis of the specimen holder. Two holograms projected from the front surface and back surface of the material were processed in order to divide the magnetic and electric fields around the specimen. Figures 2(b) and (c) are examples of reconstructed interferograms of the magnetic and electric fields. Holograms by using a double-biprism interferometer [5] for tomography were recorded every 10°. Eighteen (18) phase maps corresponding to the projected magnetic field were reconstructed from thirty-six (36) holograms. The phase maps were processed into a three-dimensional (3-D) magnetic field distribution in free space by using a modified tomography algorithm.

Figure 3 shows the reconstructed 3-D magnetic field distribution on the plane perpendicular to the pillar-shaped magnet. Figure 4 shows the reconstructed magnetic field in three planes parallel to the pillar.

In order to improve the precision and resolution of 3-D reconstructions of the magnetic field, especially inside the materials, two components of the magnetic field should be measured independently by using Eq. 1. A dual-axis 360° rotation specimen holder has already been developed for this purpose [6]. The results of using this dual-axis holder will be reported soon.

References:

[1] S. Ono et al., Appl. Phys. Express, **4,** (2011) 066601.
[2] G. Lai et al., Appl. Opt., **33,** (1994) 829.
[3] G. Lai et al., J. Appl. Phys., **75,** (1994) 4593.
[4] H. Shinada et al., IEEE Transaction on Magnetics, **28,** (1992) 1017.
[5] K. Harada et al., Appl. Phys. Lett., **84,** (2004) 3229.
[6] R. Tsuneta et al., Kenbikyou, **48,** (2013) 205 (in Japanese).

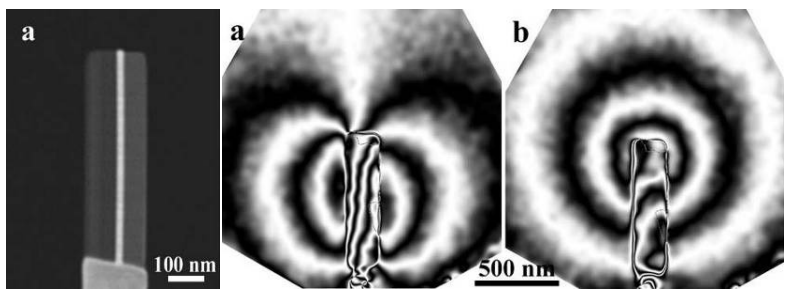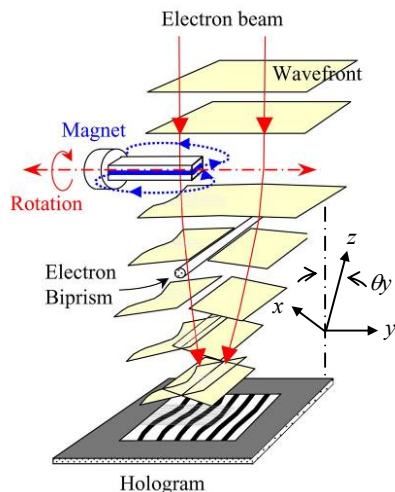**Figure 2**. (a) Scanning ion micrograph of C/CoFeB/SiO2, (b) reconstructed interferogram of magnetic field, (c) interferogram of electric field.

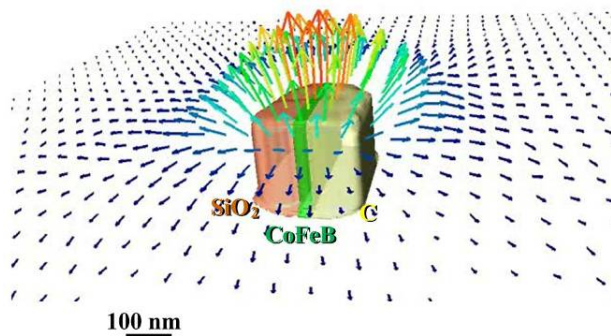**Figure 1**. Experimental setup for tomography/holography.
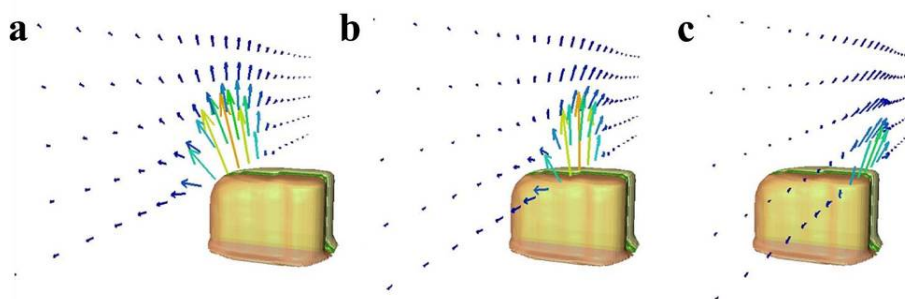

Figure 3. Reconstructed 3-D magnetic field distribution.

Figure 4. Reconstructed 3-D magnetic field distributions.